Research Article

Widespread Dispersion of Neuronal Clones Across Functional Regions of the Cerebral Cortex

CHRISTOPHER WALSH AND CONSTANCE L. CEPKO*

The cerebral cortex of the mammalian brain has expanded rapidly during the course of evolution and acquired structurally distinguishable areas devoted to separate functions. In some brain regions, topographic restrictions to cell intermixing occur during embryonic development. As a means of examining experimentally whether such restrictions occur during formation of functional subdivisions in the rat neocortex, clonally related neocortical cells were marked by retroviral-mediated transfer of a histochemical marker gene. Clonal boundaries were determined by infection of the developing brain with a library of genetically distinct viruses and amplification of single viral genomes by the polymerase chain reaction. Many clonally related neurons in the cerebral cortex became widely dispersed across functional areas of the cortex. Specification of cortical areas therefore occurs after neurogenesis.

THE CEREBRAL CORTEX REACHES ITS GREATEST SIZE AND functional complexity in primates. The cortex covers the forebrain as a folded sheet, subdivided into areas devoted to vision, sensation, audition, or other functions. Each area shows regional specialization of a basic cellular structure, comprising six neuronal layers. Furthermore, each area can be divided physiologically into smaller units, or columns, in which the six layers share anatomical connections and physiological properties.

A more primitive part of the brain, the hindbrain, develops according to a pattern analogous to the segmental development of the *Drosophila* embryo (*1*). The anlage of the future hindbrain forms segmental bulges called rhombomeres. Rhombomeres form domains that confine clones of cells (*2*) and domains of differential gene expression (*3*). It is not yet clear whether there are similar cell lineage restrictions during early development of the neocortex.

Several lines of evidence suggest that there is substantial intermingling of clones of cortical neurons during development. In experiments on chimeric mice, formed by fusion of cells from distinguishable species or strains, intermingling of cells was seen between radially oriented columns (*4*). Retroviral marking studies of the mammalian cortex have confirmed that cortical cells migrate along radial glia (*5*), as had been shown by other methods (*6*). Although Luskin and co-workers (*7*) suggested that clones remain substantially clustered, we and others have noted significant dispersion among clonally related cells during their migration (*8–10*). Dispersion seemed to be greatest in the medial-lateral plane during fetal development and continued after birth. In postnatal and adult brains, cells labeled by retroviral marking formed unpredictable, dispersed patterns, and clonal boundaries were impossible to determine accurately (*8, 10*).

It is not possible to definitely determine clonal boundaries in the adult cortex by marking cells with retroviruses because these vectors do not provide a means for distinguishing marked cells that are part of different clones (*11*). We now describe a method that allows clonal boundaries to be determined independently of patterns of migration; and we have applied this method to test the functional specification of progenitors in the cortex.

Retroviral library construction and clonal analysis by the polymerase chain reaction (PCR). A library of retroviral vectors was constructed by inserting fragments of DNA into BAG (*12*), a viral vector that contains the lacZ gene of *Escherichia coli*, which encodes β-galactosidase. These inserts function as genetic tags that can precisely identify each member of the library (*13*) (Fig. 1). Amplification of 120 constructs by PCR followed by simultaneous digestion of these PCR products with five restriction enzymes (Cfo I, Alu I, Rsa I, Msp I, and Mse I) allowed the selection of 100 viral constructs with tags that were easily distinguished from each other

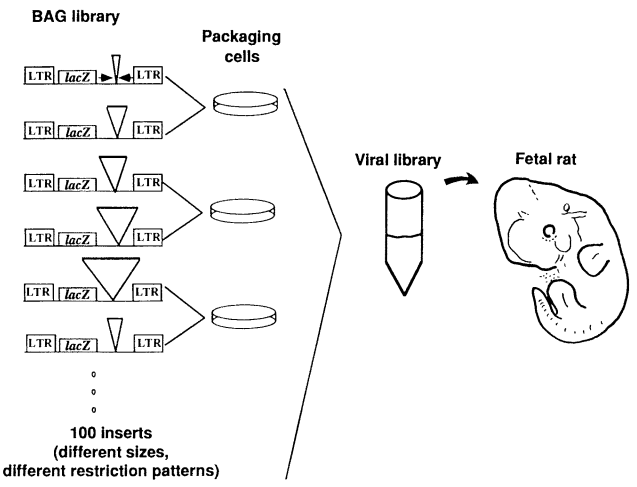

Fig. 1. Strategy for the preparation of the retroviral library. Each vector contains the *lacZ* gene and the neomycin resistance gene, as well as a short piece of unique DNA as a genetic tag. One hundred plasmid constructs were transfected pairwise to produce 50 viral supernatants. A mixture of these supernatants was injected into the brain of developing rats to label the progenitors of cerebral cortical cells and their progeny. Sites for the PCR primers are indicated by arrowheads.

C. Walsh is in the Department of Genetics, Harvard Medical School, 25 Shattuck Street, Boston, MA 02115, and the Department of Neurology, Massachusetts General Hospital, Fruit Street, Boston, MA 02114. C. L. Cepko is in the Department of Genetics, Harvard Medical School, 25 Shattuck Street, Boston, MA 02115.

*To whom correspondence should be addressed.

Table 1. Patterns of PCR-analyzed clones. N, neurons; G, glia; U, uncertain cell type; T, total; and N-G, neurons and glia. Although 597 cells have been successfully analyzed with the PCR, results from three partially analyzed brains and from clones below the cortical gray matter have been omitted from this table. Analyses of the right and left hemispheres were considered to be separate experiments. Columns indicate the number of genetic tags successfully amplified in that experiment, which is taken as a measure of the total number of clones. Neuronal clones were defined as containing at least one well-stained neuron and no glia; unidentified clones comprised cells where histochemical staining of processes was inadequate to identify the cell types. Although Figs. 2 and 6 show flattened cortical sections, similar clonal patterns were seen in brains sectioned parasagittally (E15-3, right) or frontally (E15-12, left; E15-2, right; E15-10, right). Glial clones consisted of either oligodendrocytes or astrocytes, and sometimes both (*45*).

Experiment	Age	Total clones (no.)	One cell	Clones of each type (no.)								
				Clustered			Nonclustered			Glia		
				N	U	T*	N	U	T*	G	N-G	T†
Infection at E15												
E15-12, left	E15-P3	4	1	0	0	0	3	0	3	0	0	0
E15-2, right	E15-adult	6	3	1	0	1	1	1	2	0	0	0
E15-3, right	E15-adult	7	3	0	0	0	2	0	2	1	1	2
E15-4, left	E15-P9	8	5	1	1	2	1	0	1	0	0	0
E15-13, right	E15-adult	9	5	2	0	2	2	0	2	0	0	0
E15-4, right	E15-P9	11	4	2	2	4	2	0	2	1	0	1
E15-9, left	E15-adult	15	10	1	0	1	3	0	3	1	0	1
E15-8, right	E15-adult	17	9	2	0	2	5	0	5	0	1	1
E15-8, left	E15-adult	20	7	0	1	1	2	2	4	6	2	8
E15-10, right	E15-adult	25	6	3	3	6	3	2	5	6	2	8
Total		122	53	12	7	19	24	5	29	15	6	21
Percentage		100	43	10	6	16	20	4	24	12	5	17
Infection at E17												
E17-4, left	E17-adult	2	0	0	1	1	1	0	1	0	0	0
E17-5, left	E17-adult	3	1	1	0	1	1	0	1	0	0	0
E17-3, right	E17-P10	13	6	0	1	1	0	1	1	5	0	5
Total		18	7	1	2	3	2	1	3	5	0	5
Percentage		100	39	6	11	17	11	6	17	28	0	28

*Sum of clones of neuronal and uncertain morphology. †Sum of glial clones and clones containing both neurons and glia.

(*14*). Supernatants containing these 100 retroviruses were prepared (*15*) and mixed in approximately equal ratios.

To infect and label cerebral cortical progenitor cells and their progeny, we injected serial dilutions of the retroviral library into the lateral ventricles of fetal rats either 15 or 17 days after their conception (E15 or E17). These 2 days are early and relatively late in cortical neurogenesis in the rat, which continues from about E13 until E21 (*16, 17*). Three or more days after their birth at E21 or E22 (Table 1), the animals were deeply anesthetized and perfused with fixative (*8*). The brains were removed and processed for β-galactosidase activity in order to localize the progeny of infected progenitor cells (*18*). The number and distribution of labeled cells were recorded with camera lucida drawings, photographs, and three-dimensional reconstructions (Fig. 2A).

Clonal analysis was performed by amplification of the genetic tags with PCR from each single, histochemically labeled cell (*19, 20*). Because cells derived from the same progenitor share the same tag and cells derived from different progenitors contain different tags, the tags define clones regardless of their patterns of migration. After protease digestion of pieces of tissue containing the nucleus of each labeled cell, an initial PCR reaction (46 cycles) was followed by a second PCR reaction (25 to 35 cycles) with a second oligonucleotide pair internal to the first (*21*). All amplified DNA segments were analyzed by agarose gel electrophoresis and restriction enzyme digestion, so that each recovered viral tag could be identified as one of the 100 in the original mixture. The PCR reaction usually produced a single sharp band or no product (Fig. 2B). A signal was seen for 50 to 80 percent of the histochemically labeled cells (average, 66 percent); we subsequently analyzed only these PCR-positive cells. For each clone, defined as histochemically labeled cells that showed the same genetic tag upon PCR amplification, we characterized the morphology and the topographic distribution of the cells (Table 1). More than 60 percent of cells could be identified as neurons or glia on the basis of histochemical staining for β-galactosidase (*8*), with the majority of clones containing either neurons or glia. Many of the clones (39 to 44 percent) consisted of a single PCR-positive cell (Fig. 2A, cell 6, and Fig. 2C, tags 11, 53, 59, and 68), either spatially isolated from other labeled cells or near other histochemically labeled cells for which the PCR yielded no product. Most of these single-cell clones were neurons (58 percent), while the remainder were unidentified because the histochemical reaction did not label the cell processes. Most of these unidentified cells are probably neurons, because (i) their labeled cell somata are usually the size expected for neurons, not glia; (ii) most of these cells are neurons when examined by electron microscopy (*22*) or after injection of dyes (*23*); (iii) a similar retroviral construct containing alkaline phosphatase as a histochemical marker (*24*) shows that more than 90 percent of these cells are neurons (*25*). Therefore, neuronal clones were defined as clones containing at least one definitive neuron and no definitive glial cells.

Clustered and nonclustered clones. Cortical neuronal clones formed two topographic patterns: clusters of clonally related neurons and nonclustered, or scattered, neurons. A frequency distribution of the longest dimension of neuronal clones (Fig. 3) shows a sharp peak at 1.5 mm or less, corresponding to clustered clones, with a broad shoulder (or perhaps a second mode) at a larger size, corresponding to nonclustered clones. Furthermore, the nonclustered clones sometimes consisted of arrays of two or more clusters spaced at regular intervals.

Clustered neuronal clones, defined as two or more cells (maximum cluster size was six) with the same genetic tag located within 1.5 mm or one another, generally comprised groups of cells that were each

others' nearest, histochemically labeled neighbors. A distance of 1.5 mm was chosen as an upper limit to define clusters, so that this size would approximate the mode at the smaller size in Fig. 3. Neurons in these clusters were not oriented in radial columns or "interrupted columns (7)" but instead were confined to one or two cortical laminae; well-stained neurons often showed similar morphological properties. This absence of columnar orientation might arise if infected cells in some laminae failed to express the lacZ gene. This possibility was investigated by PCR analysis of the unlabeled cortical tissue surrounding several labeled clusters. The PCR amplification revealed no evidence of proviral sequences in nearby unlabeled tissue. The laminar orientation of clustered clones is consistent with results of other studies (*4, 22, 26*), which have suggested either that pyramidal and nonpyramidal cells have distinct precursors or that upper and lower cortical layers tend to have different precursors.

Clustered neuronal clones were not limited to single functional

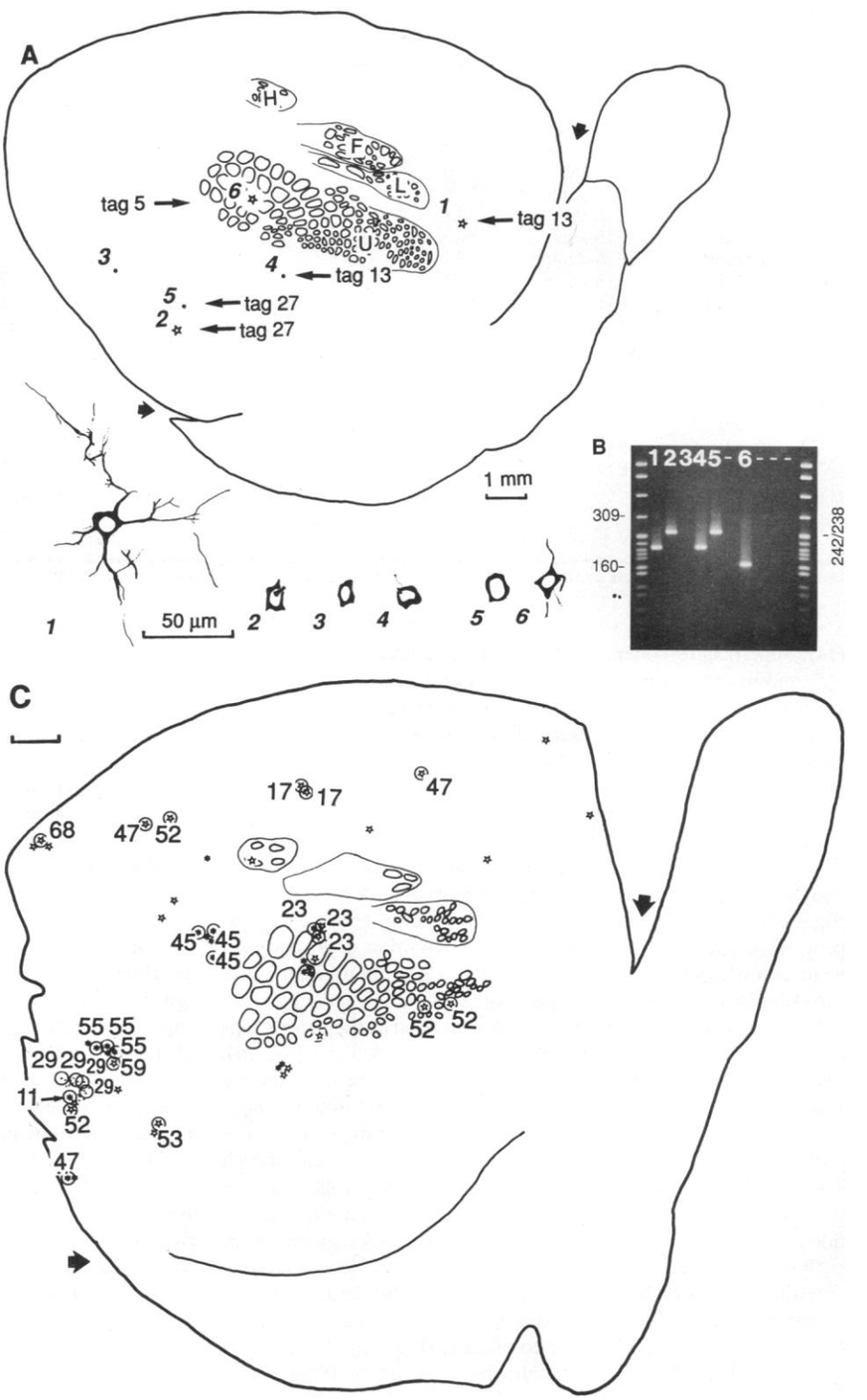

Fig. 2. PCR analysis of labeled cells. (**A**) A reconstruction of one hemisphere of the cerebral cortex and the olfactory bulb, showing the location of histochemically labeled cells after an injection of the viral library at E17 (E17-5, left; see Table 1). The cerebral cortex was sectioned parallel to the cortical layers, stained for β-galactosidase, and then for cytochrome oxidase (*27*). Superimposition of cortical landmarks, such as blood vessels and barrels, visualized by the cytochrome oxidase reaction, allowed a reconstruction in serial sections of the position of all β-galactosidase–positive cells in relation to the functional domains of the cortex. The cytochrome oxidase reaction visualizes a map of the contralateral body surface in the somatosensory area of the cortex, including representations of the upper lip and face (U), lower lip (L), forelimb (F), and hindlimb (H). In all cortical outlines, the rostral olfactory bulb is to the right, caudal is to the left, dorsal cortex is up, and ventral-lateral cortex is down. The rhinal fissure, the ventral-lateral border of the neocortex, is indicated by wide arrows. The six β-galactosidase–positive cells were plotted and drawn with a camera lucida device (below). Three cells, identified as neurons by their larger soma size and the pattern of cellular processes, are indicated by large stars (cells 1, 2, and 6); dots represent cells with an unclear phenotype (cells 3, 4, and 5). Labeled cells were then removed from the tissue sections and processed with the PCR to amplify the genetic tags. (**B**) An agarose gel stained with ethidium bromide containing PCR products from cells 1 to 6. Five cells gave a single, amplified band, while one cell (cell 3), as well as several samples of unlabeled cortical tissue (−), gave no signal. Cells 1 and 4 contained the same tag, as did cells 2 and 5; this result was confirmed with a restriction enzyme digestion. (**C**) Labeled cells in a typical experiment after an injection at E15 (E15-4, right hemisphere). Neurons are indicated by open stars, astrocytes by small dots, and cells with an unclear identity by filled stars. The rhinal fissure is indicated by a long curved line and by wide arrows. About half of the cells gave a PCR signal, and these cells are circled. Eleven distinct PCR tags were seen; cells from which they were recovered are numbered according to which tag (of the 100 in the library) was present. These 11 tags were all distinct from the three tags in the experiment in (A). The single astrocyte clone formed a very dense cluster (tag 29). Clones containing each tag were either single cells (tags 11, 53, 59, 68); clustered neuronal clones (tags 17 and 23); clustered clones in which none of the cells could be definitively identified as a neuron (tags 45 and 55); or nonclustered neuronal clones (tags 52 and 47). Clustered cells can be members of distinct clones (tags 29, 11, 52, 55, 59). Neurons carrying tag 52 cross the boundaries of barrels in the somatosensory cortex and are part of a larger clone including cells in the occipital cortex. A second nonclustered neuronal clone contains cells in occipital cortex, presumptive somatosensory cortex, and the motor cortex (tag 47). When members of the clones in caudal cortex are connected by lines drawn between nearest neighbor labeled cells carrying the same tag, both nonclustered clones share orientation between rostromedial and caudolateral cortex, although their patterns diverge further rostrally. Scale bar, 1 mm.

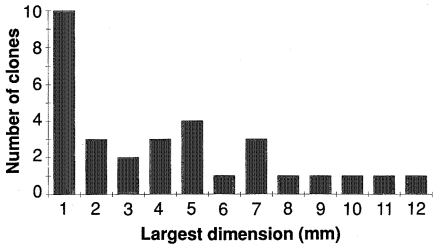

Fig. 3. Histogram of the longest dimension of each clone (that is, cells showing the same genetic tag) defined by the PCR analysis. Data are from experiments containing 17 tags or fewer, although the results were the same in brains with higher and lower densities of infection. The linear distance separating the two furthest cells was measured for each clone. Clones appeared to distribute in a bimodal fashion, with one mode at 1.5 mm or less, and a second very broad peak at a much wider range.

subdivisions of the cortex. Cytochrome oxidase histochemistry of the somatosensory cortex (*27*) reveals functional subdivisions of the somatosensory cortex, which form a systematic map of the contralateral body surface. Subdivisions, called barrels, reflect the patterns of whiskers on the face of the rat, with each barrel receiving information primarily from one whisker (*28*). Similar subdivisions in the sensory representations of the limbs correspond to single pads on the digits (*29*). We analyzed the distribution of clonally related cells relative to the barrels by double histochemistry for β-galactosidase and cyctochrome oxidase and then performed PCR analysis. Within the limited sample of four clustered neuronal clones that occurred in the barrel field (Fig. 4), none were confined to one barrel, and all clusters crossed one or more barrel boundaries. Even neutrons that were 100 μm or less apart were in separate barrels.

Although the cells in clustered clones were dispersed up to 1.5 mm, histochemically labeled cells that were within 1.5 mm of each other (or even nearest neighbors) sometimes comprised more than one clone when analyzed with the PCR, especially when these neurons were in widely separated cortical laminae (Fig. 2C and Table 2). Although such occurrences were more common in brains in which larger numbers of cells were labeled, they occurred even in brains with very few labeled cells. Thus, the pattern of histochemical labeling alone is not sufficient to determine clonal boundaries in the

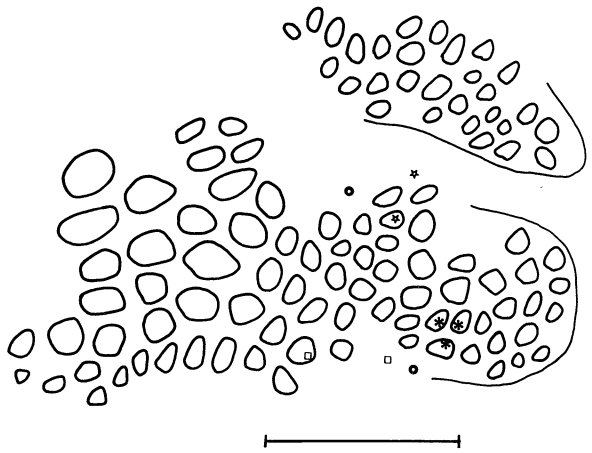

Fig. 4. Clustered clones in relation to the barrels of the somatosensory cortex. All clustered neuronal clones in the barrel field are illustrated from the six hemispheres that were sectioned and reconstructed after flattening. All of the clones occurred in the upper lip region, and they have been superimposed onto a single tracing for clarity. Relations of each clone to functional areas were determined with cytochrome oxidase staining in combination with β-galactosidase histochemistry in single sections. The lower lip representation is shown above the representation of the upper lip to preserve the overall orientation of this drawing with respect to the other figures (medial is up, rostral to the right, caudal to the left, ventrolateral is down). Some of the clustered clones were part of larger nonclustered clones (Fig. 6). Scale bar, 1.0 mm.

Table 2. Errors in assigning clonal boundaries resulting from the use of geometric criteria. A total of 78 PCR-defined clones was included in the analysis from eight experiments, after infection at E15 or E17. All brains were sectioned parallel to the cortical layers. For each experiment, clonal boundaries were drawn from the three-dimensional reconstruction of the pattern of histochemically labeled cells by using the geometric criteria of 250 μm, 500 μm, and 1000 μm as the longest dimension of putative clones. These data were then compared to the results obtained with PCR in terms of the number of clones and the errors in the assignments of these clones. Only cells that gave PCR signals were included in this analysis.

Group	Geometric criterion			
	250 μm	500 μm	750 μm	1000 μm
Clones defined geometrically (no.)	111	96	86	79
Clones incorrectly assigned (no.)				
Lumping errors (no.)	2	10	16	23
Percent of PCR-defined clones	2.6	12.8	20.5	29.5
Splitting errors (no.)	58	49	40	39
Percent of PCR-defined clones	74.4	62.8	51.3	50.0

cerebral cortex. With only histochemical labeling to determine clonal relations, both "lumping" together of cells that are members of different clones and "splitting" of clones into smaller units occur quite frequently. We were unable to develop rules, retrospectively, that would allow accurate identification of cells as siblings without the PCR analysis. Splitting errors were especially common due to the presence of very widely scattered, nonclustered clones.

Analysis of nonclustered clones. In addition to the pattern of clustered cells described above, many cells containing the same tag were scattered over large distances, sometimes approaching the largest dimension of the entire neocortex (Fig. 2A, tag 13, and Fig. 2C, tags 47 and 52). These nonclustered patterns constituted neurons, or a mixture of neurons and some unidentified cells, scattered singly or as several clusters. Two possible explanations exist for the nonclustered pattern. It is possible that, in some cases, viruses carrying a given tag infect more than one cell coincidentally. However, several lines of evidence support an alternative explanation, that is, that the majority of the nonclustered patterns represent dispersion of clonally related cells across much of the neocortex.

In order to test whether some viral tags were overrepresented in the library and thus infected several cells per experiment, we confirmed that the 100 tags originally included in the library were represented approximately equally. We tabulated the molecular size and pattern of fragments generated by restriction enzyme digestion for all PCR-analyzed tags in all experiments, and matched them to the 100 tags in the library. The members of the viral library were represented equally, and the nonclustered patterns were not seen preferentially with any particular tag (Fig. 5). Although each hemisphere that we analyzed contained 2 to 25 different tags, different experiments usually showed distinct ensembles of tags. For example, the three tags in the experiment in Fig. 2A were all different from the 11 tags in the experiment in Fig. 2C.

However, even with an equal mixture of 100 tags, there is still a significant probability that the same tag will appear more than once in a particular brain by coincidence. This problem can be modeled as sequential picks (that is, clones), with replacement after each pick, from a population with 100 members (that is, tags). Probabilities that the same member will be picked twice can be calculated from the multinomial equation (*30*) or by using a Monte Carlo computer simulation (*31*), in which picks are repeated and the summed results

of many trials are used as probabilities. One element will be picked twice with a probability of 0.03 if there are three picks, and a probability of 0.06 if there are four picks; with eleven picks, there is a probability of 0.50 that any element will be picked twice. Nonetheless, nonclustered clones were as common in lightly infected brains as in heavily infected brains: in the three brains that received extremely dilute infections (four or fewer tags per hemisphere), five of nine tags appeared in nonclustered neuronal clones, and each of the three brains showed at least one nonclustered clone. After slightly less dilute infections (4 to 11 tags per hemisphere), nine of 41 tags appeared in nonclustered patterns; in more heavily infected brains (more than 11 tags), 18 of 85 tags appeared in nonclustered patterns.

We also used the Monte Carlo simulation to calculate directly the theoretical probability that each nonclustered pattern in each experiment represents a coincidental appearance of the same tag in distinct clones (*32*). Many nonclustered clones contained three or more widely separated subunits (single cells or clusters of cells) (Fig. 2C); therefore, even in experiments where two infections by one tag are possible or even likely, three or more infections by the same tag are highly unlikely. With a criterion that the probability is less than 0.05 that a nonclustered clone could arise from multiple infections by one tag (that is, such a coincidence would occur less than once in twenty experiments), the nonclustered patterns are very common (Fig. 6); 11 nonclustered clones occurred in the ten experiments with injections at E15. Therefore, because all the experiments are independent, the probability that all or even most of the nonclustered patterns were actually not clones is minuscule.

Nonclustered clones showed nonrandom topographic patterns. For example, lines that connect the cells in all three nonclustered clones labeled at E17 (Table 1) showed the same orientation, approximately parallel to the rhinal sulcus (Fig. 2A). Nonclustered clones labeled at E15 tended to contain more cells (mean number of cells was 3.5 after E15 injection and was 2.0 after E17 injection), and some clones showed an orientation with respect to the rhinal sulcus similar to that of the E17 clones. In the caudal portion of the cortex, nonclustered clones showed an orientation that did not parallel the rhinal sulcus, but was parallel to a line running between caudolateral and rostromedial cortex. More rostrally, some clones were oriented parallel to the medial border of the cortex (Fig. 6, top). However, several other clones (Fig. 6) contained cells that were widely separated between medial and lateral regions of cortex. We do not yet know all of the cellular movements responsible for these patterns.

We conclude that the nonclustered patterns represent dispersion of clonally related cells across most or all of the neocortex. Members of nonclustered clones, even when labeled near the end of cortical neurogenesis (E17), are present in cortical areas devoted to very different functions (Fig. 2A). Clones were dispersed across the borders of the visual, somatosensory, and motor areas; the auditory, somatosensory, and motor areas (Fig. 6); and more commonly between two adjacent areas, in a fashion that does not suggest any segregation of clones within functional subdivisions of the cortex. These findings indicate that cortical neurons are not specified regarding their ultimate areal fate by a lineage-based mechanism. Functional specification must arise through mechanisms acting after neurogenesis.

Retroviral libraries and PCR for the analysis of clonal relations. Although injection of our retroviral library into developing brain can define clonal boundaries independently of pathways of migration, the efficiency of the PCR amplification is not optimal. The genetic tag is only amplified in 50 to 80 percent of cells. This figure is comparable to that obtained by amplifying single spermatozoa with a comparable cell lysis and PCR protocol (*33*), suggesting that use of fixed tissue did not compromise sensitivity of the PCR. We have found no evidence that some inserts amplify better than others (Fig. 5), and the median size of the DNA fragments amplified from fixed tissue matched the median size of the tags originally included in the library. Therefore, our sample represents a random sample of the behavior of retrovirally labeled cortical progenitors. However, because of incomplete amplification—as well as other possible variables (lack of expression of β-galactosidase, cell death, failure of the histochemical reaction) that would lead to a

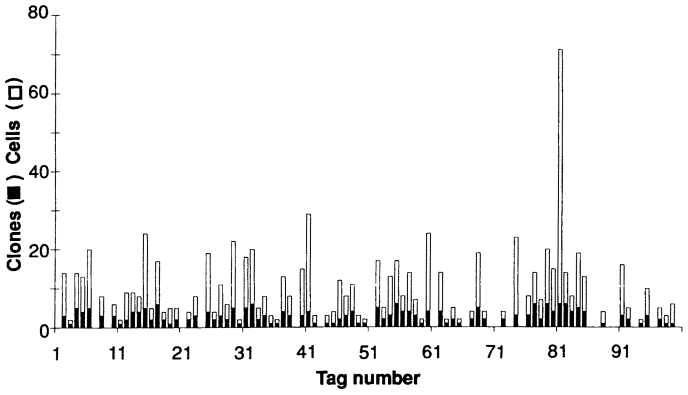

Fig. 5. Representation of genetic tags in the retroviral library. The histogram represents pooled data from 16 experiments, with a total of 597 cells and 235 clones. Tags are arranged by size and are numbered from 1 to 100 on the x axis. The y axis shows the number of experiments (that is, cerebral hemispheres) in which that tag appeared (black) and the total number of cells in which that tag was seen (open). The number of cells per tag varies widely, because it reflects differences in clone size (for example, some glial clones were very large). There was no evidence that any one label is present in excess, and no tag appeared in more than 6 of 16 experiments. Tags 13, 47, and 52, present in the nonclustered clones in Fig. 2, are not overrepresented. As expected, not all tags in the library have been recovered yet, due to the limited number of experiments completed to date.

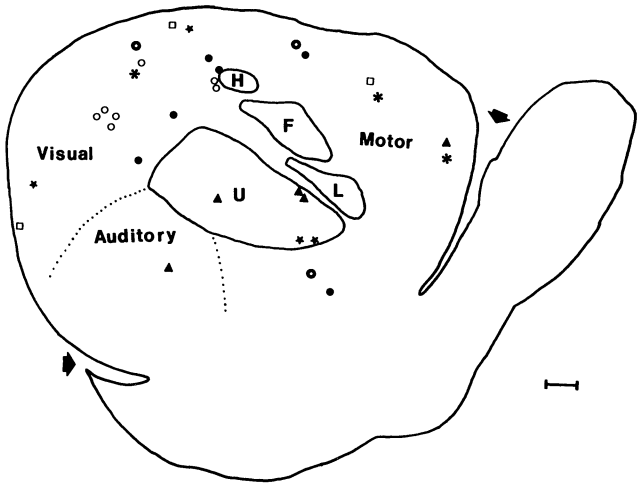

Fig. 6. Topographic patterns of nonclustered neuronal clones after infection at E15. Nonclustered clones from brains sectioned after flattening when the probability was less than 5 percent that the pattern of label could arise as coincidental multiple infections by one tag. This criterion eliminates clones containing only two nonclustered cells in heavily infected brains. Functional areas of the cortex, broadly defined, are indicated: the occipital visual cortex, the frontal motor cortex, and the ventrolateral auditory cortex surround the somatosensory cortex, which includes the representation of the upper lip (U), lower lip (L), forelimb (F), and hindlimb (H). Boundaries are approximate. Several nonclustered clones cross cytoarchitectonic boundaries: for example, motor cortex to somatosensory cortex to auditory cortex (triangles), occipital cortex to somatosensory cortex (stars and bold open circles), and visual cortex to motor cortex (open squares and asterisks). Results from six different experiments were superimposed with the use of the cytochrome oxidase visualization of the barrel field. Scale bar, 1.0 mm (*44*).

decrease in the apparent size of clones—we cannot derive accurate numbers for actual clone sizes. The PCR technique has also allowed us to show the lack of histochemical expression of β-galactosidase in neurons does not determine the patterns of clonal dispersion (*34*).

Mechanisms and functions of clonal dispersion. Several mechanisms probably contribute to the diverse patterns of cell allocation we have observed. Cortical cells are generated by mitotic progenitors in two proliferative layers deep in the brain, the ventricular zone and the subventricular zone (*35*). Postmitotic cortical neurons must ultimately migrate in a predominantly radial direction through the intermediate zone to reach the cortical plate, precursor of the cerebral cortex. Although migration seems to be supported by radial glial fibers (*5, 6*), the association of migrating cells with radial glia does not appear absolute. Radial glia fasiculate and defasiculate (*36*), and there may be exchange of migrating cells among fibers or among fasicles during the course of migration (*6*). Such an imprecise path may produce clustered clones (*11*).

The nonclustered patterns are more complex. Wide medial-lateral dispersion of clonally related cells in the rostral portion of the cortex (Fig. 6) has been suggested on the basis of [^{3}H]thymidine studies (*17, 37*), chimera experiments (*4*), and our own retroviral data (*8, 10, 11*). The medial-lateral dispersion occurs in regions where radial glial fibers are very elongated, taking circuitous routes around the basal ganglia. Cortical cells in a wide medial-lateral zone are formed mainly from a narrow proliferative zone, so that minor displacements of progenitor cells within this proliferative zone might ultimately produce wide dispersion of cells. On the other hand, the distribution of nonclustered cells in a rostral-caudal direction suggests that cells may migrate essentially parallel to the ventricular surface. One possibility is that the dividing progenitor cells migrate, since some dividing cells in the subventricular zone move in a rostral-caudal direction in cortical slices (*38*). As yet, however, the mechanisms of nonradial dispersion of cortical cells are not known.

The patterns of cell generation do not specify the later functional organization of the cortex into cytoarchitectonic areas. Neurogenesis may produce a cortex that is initially functionally equivalent, which is later sculpted into functional areas by intercellular interactions. This hypothesis has been proposed before, because (i) changes made in the whisker pattern during development can be faithfully reflected in the somatosensory cortex (*39*), (ii) auditory (*40*) or somatosensory cortex (*41*) can form functional visual units after rerouting of inputs to the thalamus, and (iii) substantial changes in neuronal morphology and connections can be produced by transplantation of developing cortex from one area to another (*42, 43*). Our data show directly that areal specification occurs after neurogenesis.

There is a potential evolutionary advantage of a nervous system in which control of cortical cell generation is independent of the later functional specification of the cortex by its afferents (*11, 42, 44*). Such a model allows fast, partially independent evolution of the cortex and the body plan, while keeping the two always coordinated. Changes in body shape could be accommodated by afferent specification of a flexible cortex, because such changes could be signaled early in development. Conversely, cortical size could change in the context of a cortex still functionally integrated with the periphery.

REFERENCES AND NOTES

1. A. Lumsden and R. Keynes, *Nature* **337**, 424 (1989); P. Hunt and R. Krummluaf, *Cell* **66**, 1075 (1991).
2. S. Fraser, R. Keynes, A. Lumsden, *Nature* **344**, 431 (1990).
3. D. Wilkinson, S. Bhatt, M. Cook, E. Boncinelli, R. Krummlauf, *ibid.* **341**, 405 (1989).
4. D. Goldowitz, *Dev. Brain Res.* **35**, 1 (1987); G. Fishell, J. Rossant, D. van der Kooy, *Dev. Biol.* **141**, 70 (1990); J. E. Crandell and K. Herrup, *Exp. Neurol.* **239**, 185 (1991).
5. J.-P. Misson, C. P. Austin, T. Takahashi, C. L. Cepko, V. S. Caviness, *Cerebral Cortex* **1**, 221 (1991).
6. P. Rakic, *J. Comp. Neurol.* **145**, 61 (1972); ———, L. J. Stensaas, E. P. Sayre, R. L. Sidman, *Nature* **250**, 31 (1984); P. Rakic, *Postgrad. Med. J.* **54**, 25 (1978); *Science* **241**, 170 (1988); U. E. Gasser and M. E. Hatten, *Proc. Natl. Acad. Sci. U.S.A.* **87**, 4543 (1990).
7. M. B. Luskin, A. L. Pearlman, J. R. Sanes, *Neuron* **1**, 635 (1988).
8. C. Walsh and C. L. Cepko, *Science* **241**, 1342 (1988).
9. J. Price and L. Thurlow, *Development* **104**, 473 (1988).
10. C. Austin and C. L. Cepko, *ibid.* **110**, 713 (1990); C. L. Cepko *et al.*, *Cold Spring Harbor Symp. Quant. Biol.* **55**, 265 (1990).
11. C. Walsh and C. L. Cepko, *Experientia* **46**, 940 (1991).
12. J. Price, D. L. Turner, C. L. Cepko, *Proc. Natl. Acad. Sci. U.S.A.* **84**, 156 (1987).
13. Genomic DNA from *Arabidopsis thaliana* was digested to completion with Mbo I, then heated to 65°C for 20 minutes to inactivate the enzyme. The DNA was then treated with 2 U of the Klenow fragment of DNA polymerase, 1 mM deoxycytosine triphosphate (dCTP), and 1 mM deoxythymidine triphosphate (dTTP) to convert the GATC termini of the DNA to TC termini. After 1 hour at 37°C, DNA was separated by size on low melting-temperature agarose, and DNA fragments less than 450 base pairs in size were isolated from the gel. The BAG vector (*12*) was digested to completion with Xho I and treated with the Klenow fragment of DNA polymerase, deoxyguanosine triphosphate (dGTP), and deoxyadenosine triphosphate (dATP) to produce GA termini. The vector was purified with agarose electrophoresis and crushed glass, treated with calf intestinal phosphatase, extracted with phenol-$CHCl_3$, and then precipitated with ethanol. Subsequently, 150 ng of vector and 15 ng of insert DNA were combined in ligation buffer with 0.5 mM adenosine triphosphate (ATP) and 2 U of DNA ligase from T4, and allowed to react overnight at 14°C. The ligation mixture was used to transform competent *E. coli* cells of the DH5 α strain. Transformed cells were grown overnight on LB medium containing kanamycin sulfate at 30 μg/ml, producing about 2000 colonies.
14. Colonies (120) were picked with sterile toothpicks, suspended in 50 μl of 50 mM tris buffer (pH 8.0) and 0.5 percent Triton X-100, and heated at 95°C for 12 minutes. Samples (10 μl) were then used as templates in 50-μl PCR reactions, which contained 10 mM tris (pH 8.3), 1.5 mM $MgCl_2$, 50 mM KCl, 0.1 percent gelatin, oligonucleotides PBR-4 (5′-GCGGAGCCTATGGAAAAACGCCAGC-3′) (0.2 μm) and BND-3 (5′-TGAGTGGCCATTAGAGCAGTAGTCCCT-GTTC-3′) (0.2 μm), 200 μM of dATP, dCTP, dGTP, and dTTP, and 1.25 U of Taq polymerase (Perkin-Elmer). Thirty-five PCR cycles (92°C for 45 seconds, 60°C for 45 seconds, 72°C for 2 minutes) were completed on a thermal cycler (MJ Research), and the products were analyzed on agarose gels. Samples (20 μl) of each PCR product were added to 3 μl of 10× buffer [100 mM $MgCl_2$, 500 mM NaCl, 10 mM dithioerythritol, and 100 mM tris buffer (pH 7.5)], 3 U each of Mse I, Msp I, Rsa I Alu I, and Cfo I, and distilled water to a final volume of 30 μl. After digestion for 2 to 16 hours at 37°, samples were analyzed on 3%/1% NuSieve-SeaKem agarose gels.
15. Retroviral vectors were prepared from these 100 constructs by transfecting "mini-prep" DNA [T. Maniatis, E. F. Fritsch, J. Sambrook, *Molecular Cloning: A Laboratory Manual* (Cold Spring Harbor Laboratory, Cold Spring Harbor, NY, 1982)], purified with crushed glass, into packaging cell lines [C. L. Cepko, in *Neuromethods: Molecular Neurobiology*, A. A. Boulton *et al.*, Eds. (Humana Press, Clifton, NJ, 1989), vol. 16]. DNA samples were transfected pairwise into 50 dishes of the ψCRIP amphotropic packaging line [O. Danos and R. C. Mulligan, *Proc. Natl. Acad. Sci. U.S.A.* **85**, 6460 (1988)] in the presence of calcium phosphate. Each supernatant was used to infect a dish of the ecotropic packaging cell line, ψ2 [R. Mann, R. C. Mulligan, D. Baltimore, *Cell* **33**, 153 (1983)] in order to make stable producer cell lines. The producer cells were selected by growth in medium containing G418 for 7 to 10 days, and the population of resistant colonies was raised to confluence. Insertion of the tags did not interfere with expression of the lacZ and neomycin resistance genes of the BAG vector. Viral supernatants were recovered and quantified on NIH 3T3 cells. Subsequent PCR amplification of DNA from infected NIH 3T3 cells confirmed the maintenance of the genetic tags in cells infected with virus. Approximately equal numbers of infectious units from each of the viral constructs were then mixed, concentrated, and stored at −70°C.
16. M. Berry and A. W. Rogers, *J. Anat.* **99**, 691 (1965).
17. J. Altman and S. A. Bayer, *Neocortical Development* (Raven Press, New York, 1991).
18. The flattened hemispheres were sectioned at 95 μm, and the sections were floated into phosphate-buffered saline (PBS) containing 2 mM $MgCl_2$. Floating sections were processed for β-galactosidase histochemistry (*8*). After the sections were rinsed in PBS three times, they were processed for cytochrome oxidase histochemistry (*27*) and rinsed twice in 5 mM tris buffer (pH 8.0) with 1 mM EDTA; cover slips were then applied with Gelvatol.
19. E. S. Kawasaki, in *PCR Protocols*, M. A. Innis, D. H. Gelfand, J. J. Sninsky, T. J. White, Eds. (Academic Press, San Diego, 1990), p. 146–152.
20. The PCR analysis was performed by removing the cover slips from the slides in sterile distilled water and dissecting small fragments of tissue containing the nucleus of each labeled cell. Fragments 50 to 200 μm in each dimension and containing ≤1000 cells were transferred to wells of a 96-well microtiter dish containing 10 μl of a solution of proteinase K (200 μg/ml), 0.5% Tween-20, and 1 μM each of the oligonucleotides PBR-5 (5′-CGGGTTTCGCCACCTCTGACTTGAGCGTCG-3′) and BND-4 (5′-TGTACTGCGGCTTGGAGCTGCTGGAATTGC-3′) in 1× PCR buffer [10 mM tris buffer (pH 8.3), 50 mM KCl, 2.5 mM $MgCl_2$, 0.1% gelatin]. The solutions were covered with 100 μl of mineral oil and incubated at 65°C for 90 minutes, 85°C for 20 minutes, then 95°C for 5 minutes. Reagents were added to achieve a final concentration of 10 mM tris buffer, 1.7 mM $MgCl_2$, 0.1-percent gelatin, 50 mM KCl, 100 to 200 μM each of dATP, dTTP, dCTP, and dGTP, each primer at 1 μM, and 0.75 U of Amplitaq DNA polymerase (Perkin-Elmer), in 30 μl of solution. The mixture was heated to 93°C for 3 minutes, then

cycled at 92°C for 30 seconds, 60°C for 3 minutes, 72°C for 10 seconds (11 times); then 92° for 30 seconds, 60° for 2 minutes, 72° for 10 seconds (35 times); then 72° for 5 minutes. Samples (4 μl) of this first reaction were used as template in a second PCR reaction with 0.2 μM each of PBR-4 and BND-3 oligonucleotides, which represent a nested pair internal to the first pair. These second PCR reactions were run for 25 to 35 cycles. All PCR products were processed for agarose electrophoresis and restriction enzyme digestion (*14*). Several precautions were taken to prevent contamination of the PCR reactions, which might have produced spurious apparent clonal relations. The tissue samples and PCR reagents were assembled in a separate, dedicated laboratory on a different floor from where the PCR products were analyzed. The thermal cycler was at yet a third location. Reagents, instruments, and glass microscope slides were irradiated with ultraviolet light to destroy possible contaminating DNA. The library was designed so that contamination from BAG plasmid (present in less than 10 percent of all samples and absent in recent experiments) did not interfere. Negative controls in every experiment included wells with unlabeled cortical tissue from the experimental brain (average, 4.5 per experiment) and wells with no added tissue (average, 7 per experiment). One unlabeled tissue control (1.7 percent of the total) showed a positive signal, and one reagent control (1.3 percent) showed a positive signal; both of these positives occurred in the same experiment (E15-10, right). Elimination of this experiment would not affect the results.

21. K. B. Mullis and F. A. Faloona, *Methods Enzymol.* **155**, 335 (1989).
22. J. G. Parnevelas, J. A. Barfield, M. B. Luskin, *Soc. Neurosci. Abst.* **16**, 1272 (1990).
23. E. A. Grove and J. Price, *ibid.* **17**, 11 (1991).
24. Human placental alkaline phosphatase, a membrane-bound enzyme, provides superior staining of neuronal processes [S. Fields-Berry, A. Halliday, C. L. Cepko, *Proc. Natl. Acad. Sci. U.S.A.*, in press].
25. C. Walsh and C. L. Cepko, unpublished results.
26. L. A. Krushel, J. G. Johnston, G. Fishell, D. van der Kooy, *Soc. Neurosci. Abstr.* **15**, 598 (1989).
27. M. T. T. Wong-Riley and C. Welt, *Proc. Natl. Acad. Sci. U.S.A.* **77**, 2333 (1980).
28. C. Welker, *J. Comp. Neurol.* **166**, 173 (1976).
29. D. D. Dawson and H. P. Killackey, *ibid.* **256**, 246 (1987).
30. R. V. Hogg and A. T. Craig, *Introduction to Mathematical Statistics* (Macmillan, New York, 1978), p. 96.
31. The Monte Carlo simulation repeated (1,000 to 100,000 times) k random picks (corresponding to k clones), with replacement, from a population with 100 elements that are equally represented, corresponding to 100 viral vectors. Simulations were then summed according to whether any one of the 100 elements were picked twice, three times, four times, et cetera. Frequencies of chance occurrence of such coincidental pairs, triplets, quadruplets, . . . were then directly computed from these sums and were used as probabilities. In test cases, the Monte Carlo and multinomial calculations gave identical results. However, since the multinomial calculation is time-consuming, a computer program that performed a Monte Carlo simulation was used routinely.
32. The following simulation was used for the experiment in Fig. 2C. We assumed that all tags were equally represented in the library and that each widely separated single cell or cluster of cells 1.5 mm or less apart was a different clone. This calculation subdivides the nonclustered patterns into several units, counted as separate clones. For example, in Fig. 2C cells carrying tags 47 and 52 would be regarded as three clones each, rather than one, giving a total of fifteen "clones." Using the Monte Carlo simulation, one can then calculate the probability that any one of 100 distinct labels will appear twice, three times, or more times, in 15 picks from the library. This probability is approximately 0.70 that one of the 100 tags will coincidentally appear twice in such an experiment, but the probability is 0.047 for the appearance of any tag three times. For the situation in which two such labels will each occur three times, the probability is less than 0.0006. Thus, for any given nonclustered pattern, there is a small probability that it represents two clones, but an extremely high ($P > 0.95$) likelihood that at least two of the widely scattered cells or clusters are part of the same clone.
33. H. Li *et al.*, *Nature* **335**, 414 (1988).
34. Unlike the neuronal clones, some glial clones and olfactory bulb clones did show lack of expression of β-galactosidase. About 10 percent of pieces of unlabeled tissue adjacent to these clones showed amplification of the same tag that was present in nearby histochemically labeled cells.
35. Boulder Committee, *Anat. Rec.* **166**, 257 (1972).
36. J.-P. Misson, M. A. Edwards, M. Yamamoto, V. S. Caviness, *Dev. Brain Res.* **4**, 95 (1988).
37. J. Altman and S. A. Bayer, *Exp. Neurol.* **107**, 36 (1990); S. A. Bayer, J. Altman, X. Dai, L. Humphreys, *J. Comp. Neurol.* **307**, 487 (1991).
38. M. W. Cooper *et al.*, *Soc. Neurosci. Abst.* **15**, 808 (1989).
39. H. Van der Loos and T. A. Woolsey, *Science* **179**, 395 (1973); T. A. Woolsey and J. R. Wann, *J. Comp. Neurol.* **170**, 53 (1976).
40. M. Sur *et al.*, *Science* **242**, 1437 (1989).
41. D. O. Frost and C. Metin, *Nature* **317**, 162 (1985).
42. D. D. M. O'Leary and B. B. Stanfield, *J. Neurosci.* **9**, 2230 (1989); B. Schlagger and D. D. M. O'Leary, *Science* **252**, 1556 (1991).
43. Unlike transplants from one neocortical area to another, similar transplants between limbic cortex and neocortex are more resistant to respecification [M. F. Barbe and P. Levitt, *J. Neurosci.* **11**, 519 (1991)], suggesting that this distinction arises earlier in neurogenesis.
44. S. K. McConnell, *Brain Res. Rev.* **13**, 1 (1988); D. D. M. O'Leary, *Trends Neurosci.* **12**, 400 (1989).
45. E. F. Ryder, C. Walsh, C. L. Cepko, *Soc. Neurosci. Abstr.* **14**, 892 (1988).
46. We thank A. Konieczny and F. Ausubel for the *Arabidopsis* DNA; G. M. Church and D. Deitcher for advice on the library; C. Tabin and P. Leder for providing a PCR laboratory; J. Hirschhorn and E. Ryder for statistical expertise; G. M. Church for use of a PCR machine and for the Monte Carlo computer simulation; and R. W. Guillery, J. G. Seidman, T. Vogt, and members of the Cepko laboratory for constructive comments on the manuscript. Research was supported by NIH grant NS 23021 (C.L.C.) and by the Dana Foundation and a Physician Postdoctoral fellowship from the Howard Hughes Medical Institute (C.W.).

16 September 1991; accepted 6 December 1991